International Journal of Applied Mathematics
Volume 38 No. 5s, 2025
ISSN: 1311-1728 (printed version); ISSN: 1314-8060 (on-line version)

# A STUDY ON THE VIBRATION AND FORCE CHARACTERISTICS OF UNMANNED AERIAL VEHICLES

**Vishwaretha K R[1*], Praveen Shenoy[2], Dr. Rajesh[3], V Madhanraj[4], Amar Gandge Subash[5]**

[1,4,5]Department of Aeronautical Engineering, Mangalore Institute of Technology & Engineering, Moodabidri ,574225
[2,3]Department of Aeronautical Engineering, Srinivas Institute of Technology, Valachil Mangalore-574143

***Corresponding Author:** Vishwaretha K R
*Email: k.vishu1994@gmail.com

## ABSTRACT

The main purpose of this research is to analyze the vibrations and forces on the drone. The project involves building a quadcopter drone and conducting test to measure the vibration and force it causes in various types of flight. Sensor like accelerometer is used to measure the frequencies of vibration. This study begins with a comprehensive review of the available literature on Drone vibrations and forces and their effects on drone performance. This literature review provides a theoretical framework and serves as a framework for experimental research. The design and construction of drones involves the selection of appropriate materials, consideration of aerodynamic properties, and the use of common damping techniques to minimize external interference. The Design and force analysis of a drone is conducted using Fusion 360. The objective of this mini project is to analyze forces experienced by a drone's components and frame during flight. Fusion 360 offers a comprehensive set of tools and functionalities for designing and simulating mechanical systems, making it an ideal platform for this analysis. The project involves creating a 3D model of the drone, applying appropriate materials and physical properties, and simulating different flight scenarios to evaluate its performance under varying conditions. The vibration analysis of a drone to assess the impact of vibrations on its structural integrity and flight characteristics. The project aims to identify the vibration sources, measure the vibration levels, and propose suitable solutions to minimize their adverse effects.

## 1 INTRODUCTION

Drones have gained significant attention in various fields, including surveillance, aerial photography, package delivery, and scientific research. As drones continue to evolve and find new applications, it becomes crucial to understand their dynamic behavior and performance characteristics. One key aspect of their performance is the analysis of vibrations and forces they experience during flight. Vibration analysis plays a critical role in assessing the structural integrity, stability, and performance of drones. Excessive vibrations can lead to reduced efficiency, decreased flight stability, and even structural failure. Understanding the vibration modes and their effects is essential for optimizing the design, improving flight performance, and ensuring the safety of drones. Similarly, the forces acting on a drone, such as thrust, drag, and lift, have a direct impact on its maneuverability, stability, and payload capacity. Accurate force analysis is necessary for predicting flight behavior, optimizing control algorithms, and designing efficient propulsion systems.

This project report aims to investigate and analyze the vibration and force characteristics of a drone. Through experimental testing and data analysis, we aim to identify and understand the vibration modes, quantify the forces acting on the drone, and evaluate their impact on flight performance. By gaining insights into these aspects, we aim to contribute to the optimization of drone design and enhance their overall performance. The report begins with a comprehensive literature review, highlighting the existing research and studies related to vibration and force analysis of drones. It

Received: August 14, 2025 

ISSN: 1311-1728 (printed version); ISSN: 1314-8060 (on-line version)

establishes the theoretical background and provides a basis for the experimental work conducted in this project. The methodology section outlines the experimental setup, data acquisition process, and analysis techniques employed. The subsequent sections focus on vibration analysis and force analysis of the drone. Vibration analysis involves the identification and characterization of vibration modes, while force analysis assesses the static forces acting on the drone during flight. Vibration analysis aims to evaluate the integrity and stability of the drone's structure under various operating conditions.
The project report concludes with a summary of the key findings, limitations of the study, and recommendations for future work. By conducting this analysis, we aim to contribute to the broader understanding of drone dynamics and assist in the development of more efficient and reliable drone systems.
Overall, this project report serves as a valuable resource for researchers, engineers, and enthusiasts interested in the vibration and force analysis of drones. The findings presented herein provide valuable insights into the behavior and performance characteristics of drones, paving the way for advancements in drone design, operation, and applications.

## 2. SELECTION OF MATERIAL

This process thus helps to choose the best material that augments your designs durability, performance and output. Ideal material selection is crucial to ensure that the product does not succumb to extreme conditions and performs well in unpredictable conditions. **PETG** (Polyethylene Terephthalate Glycol) is a popular thermoplastic that offers several beneficial properties suitable for drone applications possesses excellent mechanical properties, including good tensile strength, impact resistance, and stiffness. These properties are essential when analyzing vibrations and forces acting on the drone, as they contribute to the structural integrity and response of the components. PETG is a lightweight material, which is desirable for drones as it helps in achieving better flight performance, agility, and maneuverability. It allows for reduced weight on the overall system, resulting in improved efficiency and payload capacity. PETG is widely available and can be easily processed using common manufacturing techniques such as 3D printing or injection molding. This availability and ease of processing make it convenient for fabricating drone components for experimental testing and analysis.
Density of the material is 1.38g/cc, Tensile Strength is 57-75Mpa, Young’s modulus is 2800-3100MPa, Thermal conductivity is 0.15-0.24W/m-K.

## 3. DESIGN USING FUSION 360

Designing a drone by utilizing Autodesk Fusion 360, a 3D CAD/CAM software, for the design of the drone's components. Fusion 360 offers tools and features that enable engineers and designers to create precise, efficient, and functional drone designs. Here are some key points to consider regarding the design process of a drone using Fusion 360.

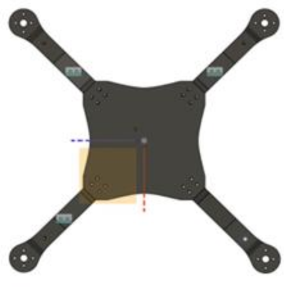

**Figure 1:Top view of drone**

**Figure 2: Side view of drone**

## 4. FABRICATION OF DRONE

The 3D printer with the chosen material and ensure it is calibrated properly. Load the 3D model files into the slicing software associated with the 3D printer. Adjust the print settings, such as layer height, print speed, and infill density, to achieve the desired balance between print quality and print time. Start the printing process and monitor it to ensure successful and accurate fabrication of each component. Once the printing is complete, remove the printed components from the build plate. Depending on the material and desired finish, post-processing steps may include removing support structures, sanding or smoothing the surfaces, and applying any necessary treatments like priming or painting. Assemble the 3D-printed components, following the design specifications and instructions.

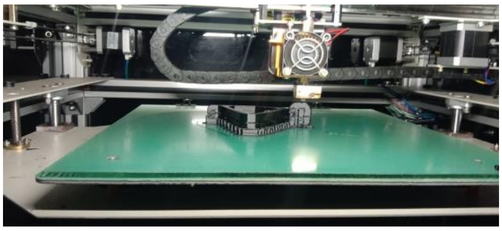

**Figure 3:** 3D Printing

## 5.COMPONENTS

**Motor:** The speed of motor is 2300RPM per 1 volt supply and it can generate about 1024 gm amount of thrust. The compatible batteries for the motor is 3S or 4S.
**Flight Controller:** The type of fight controller is F405 V1.1. The processor used for the flight controller is ARM STM32F405RGT6. It accepts 11.1 volts from 3-6s Li-po battery.
**Propeller:** The material used for the propeller is Glass Fiber Nylon. The length of the propeller is 6inch and the pitch of propeller is 4.5inch.

**Theoretical thrust calculation**

$T= [(\Pi*p)^2*(2\ \pi R^2\ \rho)]^{1/3}$ in N
Radius of propeller (R)=0.0762m
Voltage (V)=12v,
Current (I) =11amps
Motor efficiency =0.75
1.Power (P)=V*I*motor efficiency
=12*11*0.75
=99watt
2.$T=[(0.75*99)^2*2*3.14*(0.0762)^2*1.25^3$
= 6.269N
For 4 motors: quadcopter
4*6.269 = 25.076N

**International Journal of Applied Mathematics**
**Volume 38 No. 5s, 2025**
ISSN: 1311-1728 (printed version); ISSN: 1314-8060 (on-line version)

**Total thrust =2.5kg.**

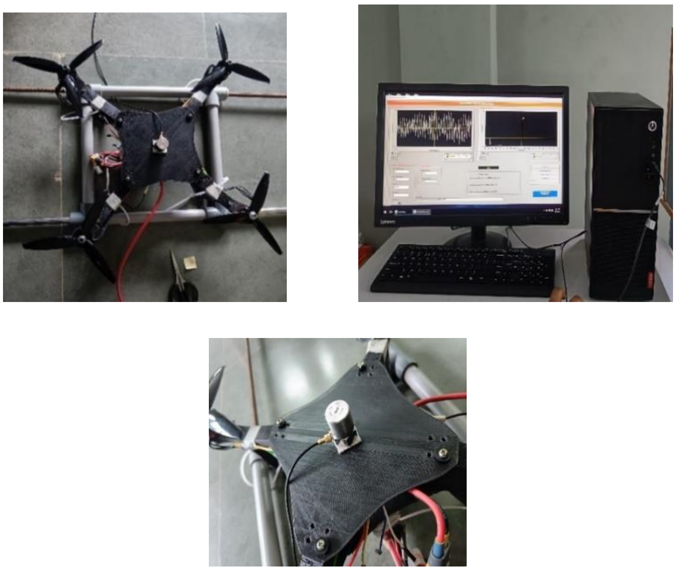

**Figure 4: vibration setup**

## 6. RESULT AND DISCUSSION

### FORCE ANALYSIS

**Table 6.1: Input to software**

| **Input to software** | |
|---|---|
| Young's Modulus | 2758 MPa |
| Poisson's Ratio | 0.35 |
| Yield strength | 70.4 MPa |
| Ultimate tensile strength | 75.7 MPa |

### 6.1Four arm:

**Table 6.2: Result of single arm**

| **Load(N)** | **Displacement(mm)** | **Stress (MPa)** | **Strain** |
|---|---|---|---|
| 1 | 0.07623 | 0.4659 | 2.277 |
| 2 | 0.1525 | 0.9139 | 4.554 |
| 3 | 0.2287 | 1.398 | 6.831 |
| 4 | 0.3049 | 1.864 | 9.108 |
| 5 | 0.3811 | 2.33 | 0.001138 |

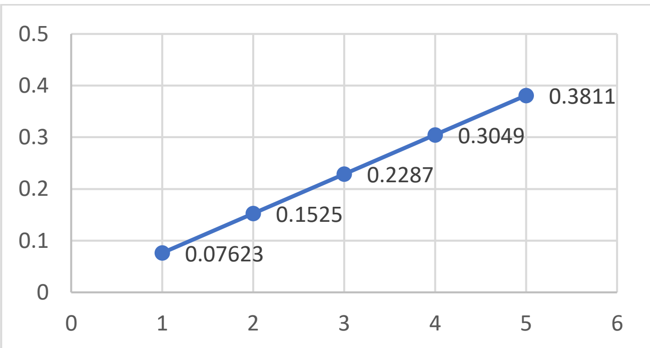


**Graph 6.1: Load v/s Displacement**

The graph 6.1 represents the load in the X-axis and the displacement in the y axis. By varying the

**International Journal of Applied Mathematics**
**Volume 38 No. 5s, 2025**
ISSN: 1311-1728 (printed version); ISSN: 1314-8060 (on-line version)

load from 1N to 5N the reading has been taken and the graph is plotted.

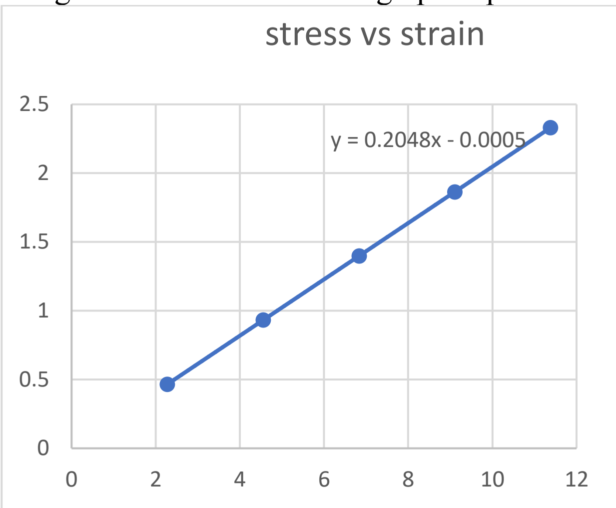


**Graph 6.2: Stress vs strain**

The graph 6.2 represents the stress in the X-axis and the strain in the y axis .by varying the load from 1N to 5N the reading has0 been taken and the graph is plotted.

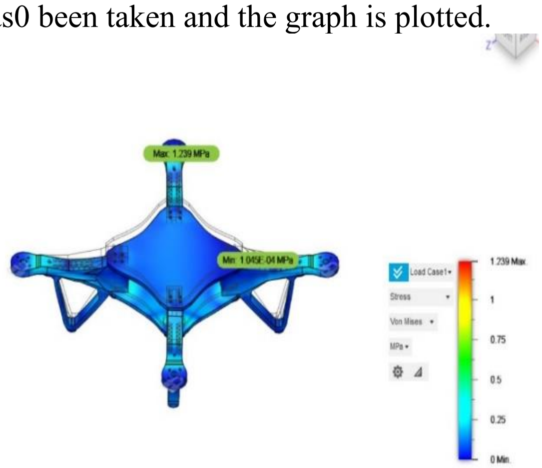

**Figure 5: Stress with payload**

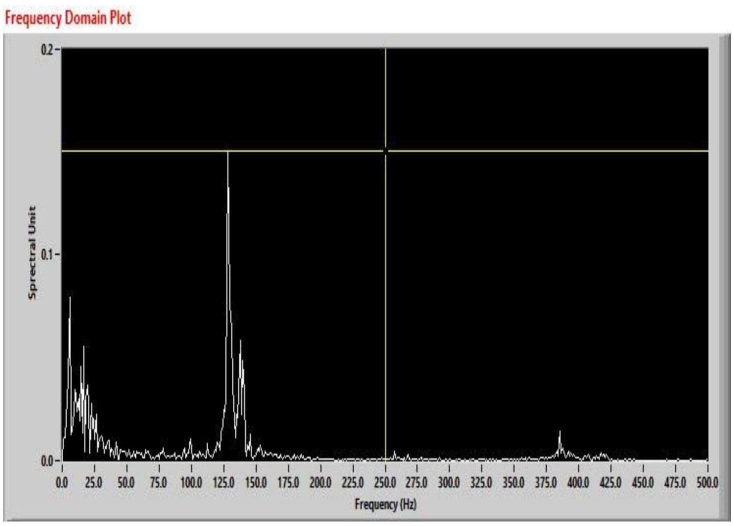


Received: August 14, 2025

International Journal of Applied Mathematics
Volume 38 No. 5s, 2025
ISSN: 1311-1728 (printed version); ISSN: 1314-8060 (on-line version)

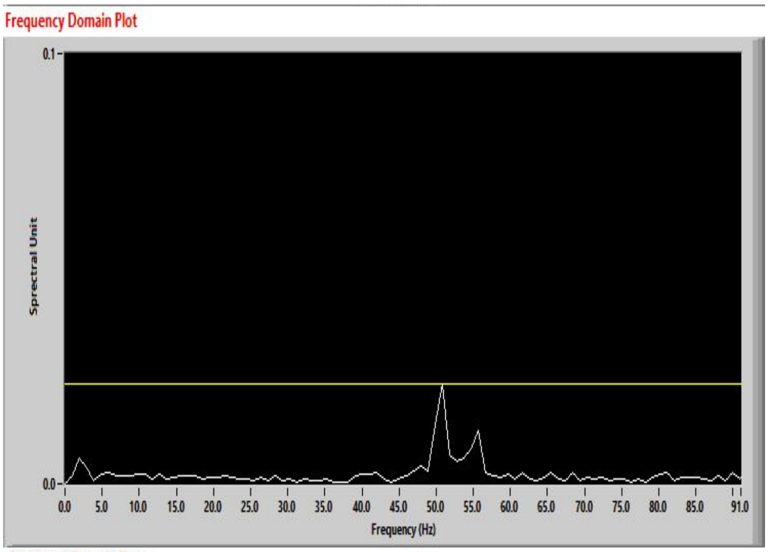


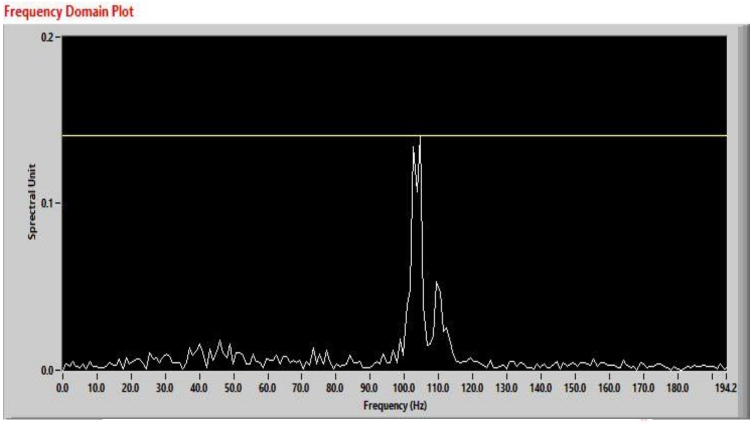


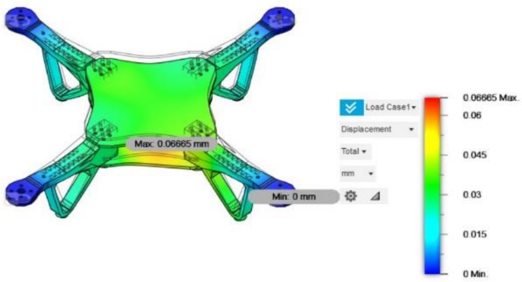


**Figure 6: Displacement with payload**

## 6.2 VIBRATION ANALYSIS

### WITHOUT DAMPER FREQUENCY

The natural frequency is typically expressed in units of frequency, such as Hertz (Hz), and represents the number of complete oscillations the system undergoes per unit of time. It is influenced by the system's physical properties, such as the mass distribution, structural stiffness, and the presence of any damping elements.

ISSN: 1311-1728 (printed version); ISSN: 1314-8060 (on-line version)

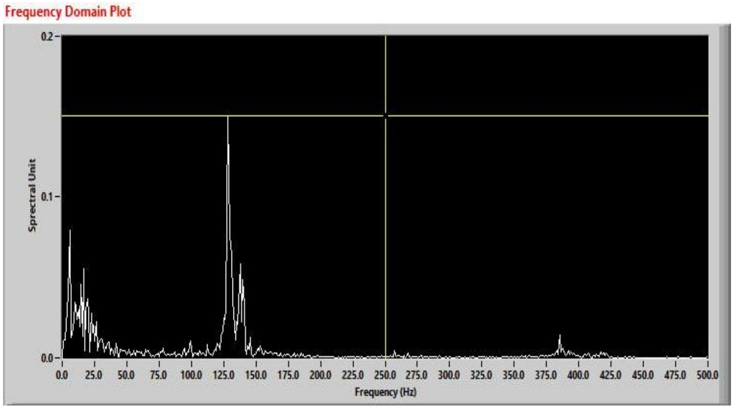


**Figure 7: Graph of Natural Frequency vs speed (RPM)**

The figure 7 represents the frequency domine plot corresponding to the Motor speed of 1100RPM. And the peak value representing the natural frequency of the drone at corresponding speed i.e.,50.8Hz.

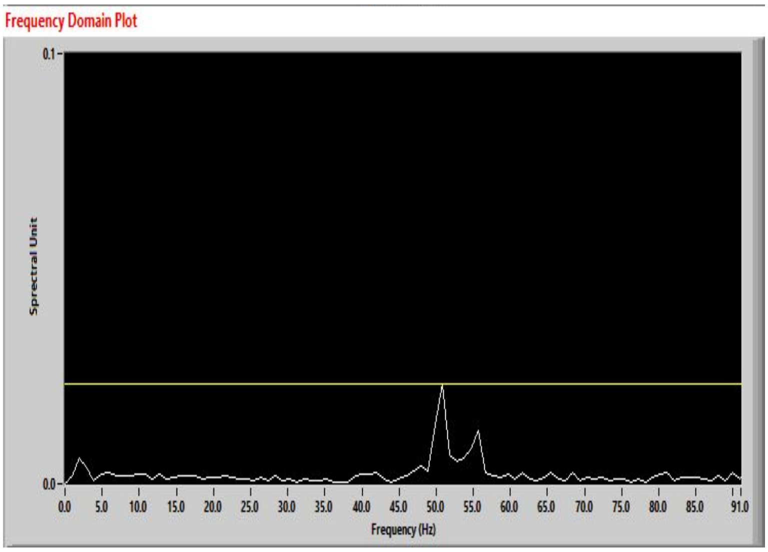


**Figure 8: Graph of Natural Frequency vs speed (RPM)**

The fig 8 represents the frequency domine plot corresponding to the Motor speed of 1250RPM. And the peak value representing the natural frequency of the drone at corresponding speed i.e.,104.6Hz.

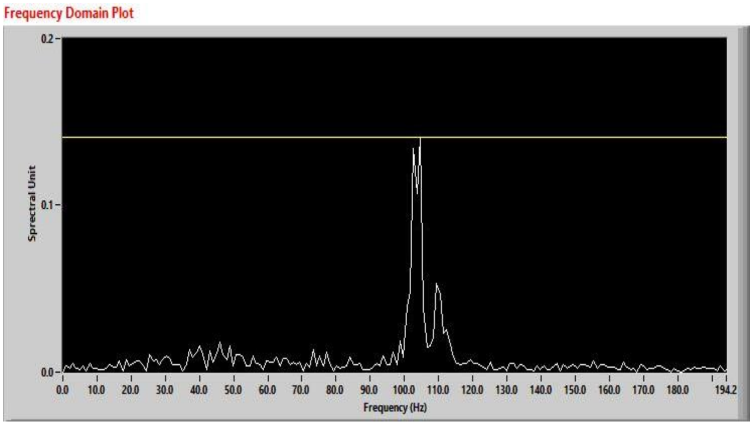


**Figure 9: Graph of Natural Frequency vs speed (RPM)**

International Journal of Applied Mathematics
Volume 38 No. 5s, 2025
ISSN: 1311-1728 (printed version); ISSN: 1314-8060 (on-line version)

The fig 9 represents the frequency domine plot corresponding to the Motor speed of 150RPM. And the peak value representing the natural frequency of the drone at corresponding speed i.e.,128.1Hz.

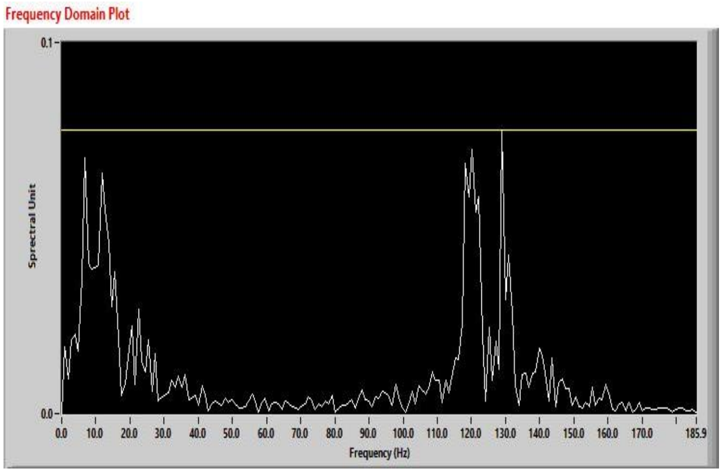


**Figure 10: Graph of Natural Frequency vs speed (RPM)**

The fig 10 represents the frequency domine plot corresponding to the Motor speed of 1450RPM. And the peak value representing the natural frequency of the drone at corresponding speed i.e.,129Hz.

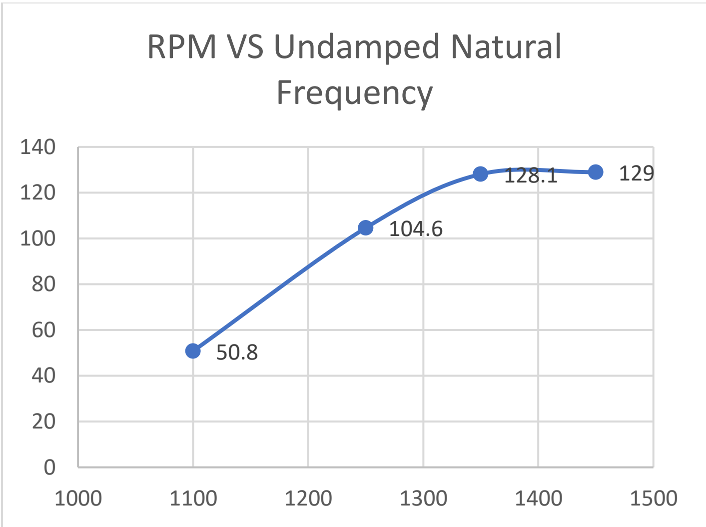


**Graph 6.5: RPM vs Natural frequency**

The graph 8.5 represents the rpm in x-axis and natural frequency in y axis. For different value of rpm, the corresponding natural frequencies are noted and the curve is obtained as shown above, the curve goes on increasing and it reaches a certain level above which the frequency becomes constant for further increase in RPM.

**DAMPED FREQUENCIES:**

The damped natural frequency is less than the undamped natural frequency, but for many practical Cases the damping ratio is relatively small and hence the difference is negligible. Therefore, the damped and undamped description are often dropped when stating the natural frequency (e.g. with 0.1 damping ratio, the damped natural frequency is only 1% less than the undamped).

International Journal of Applied Mathematics
**Volume 38 No. 5s, 2025**
ISSN: 1311-1728 (printed version); ISSN: 1314-8060 (on-line version)

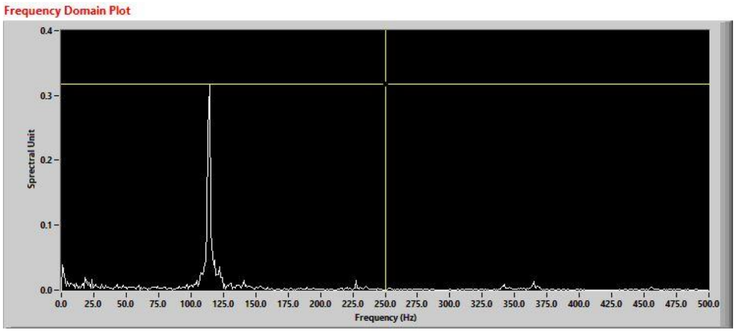


**Figure 11: Graph of Damped Natural Frequency vs speed** (RPM)

The fig 12 represents the Damped frequency domine plot corresponding to the Motor speed of 1100RPM. And the peak value representing the damped natural frequency of the drone at corresponding speed i.e.,40.1Hz.

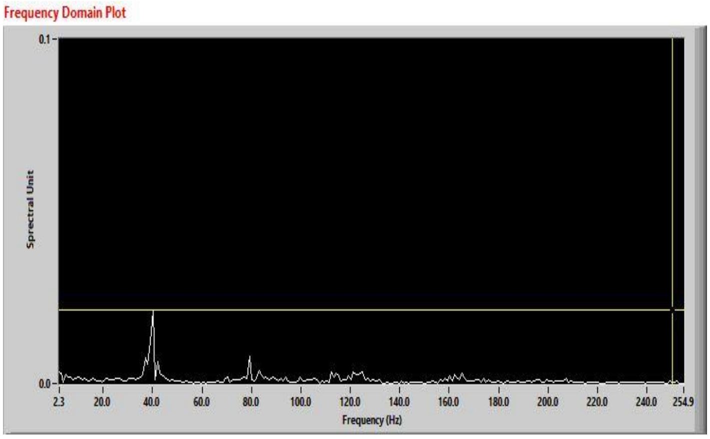


**Figure 12: Graph of Damped Natural Frequency vs speed (RPM)**

The fig 12 represents the Damped frequency domine plot corresponding to the Motor speed of 1250RPM. And the peak value representing the damped natural frequency of the drone at corresponding speed i.e.,94.8Hz.

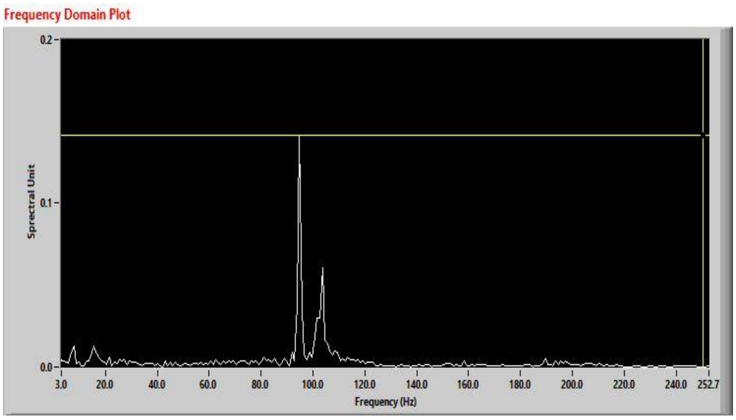


**Figure 13: Graph of Damped Natural Frequency vs speed (RPM)**

The fig13 represents the Damped frequency domine plot corresponding to the Motor speed of 1350RPM. And the peak value representing the damped natural frequency of the drone at corresponding speed i.e.,114.8Hz.

International Journal of Applied Mathematics
Volume 38 No. 5s, 2025
ISSN: 1311-1728 (printed version); ISSN: 1314-8060 (on-line version)

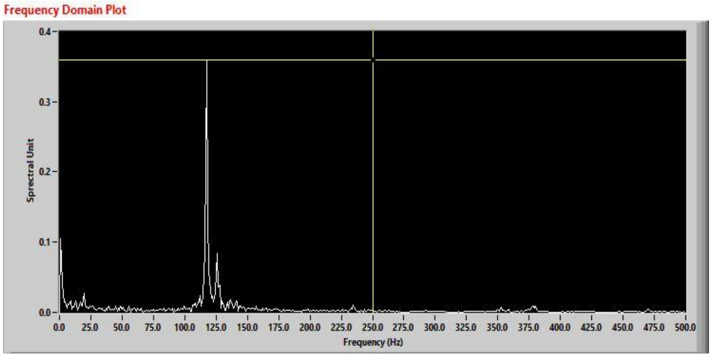


**Figure 14: Graph of Damped Natural Frequency vs speed (RPM)**

The fig 14 represents the Damped frequency domine plot corresponding to the Motor speed of 1450RPM. And the peak value representing the damped natural frequency of the drone at corresponding speed i.e.,117.8Hz.

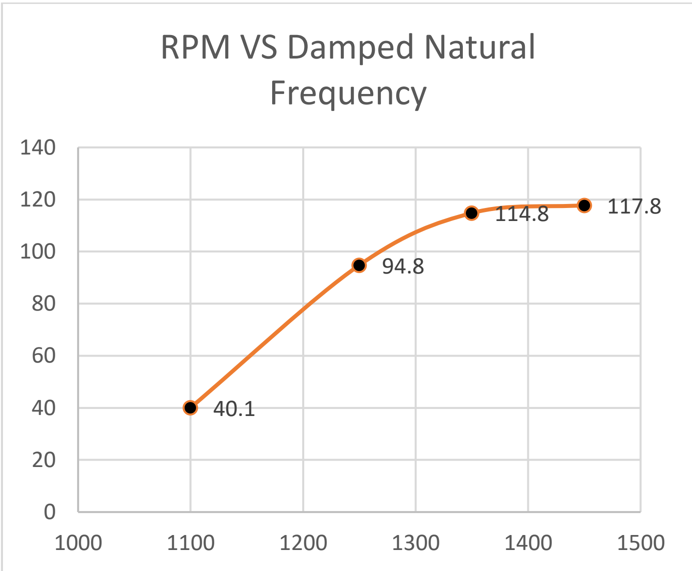


**Graph 6.6:RPM vs Damped natural frequency**

The graph 6.6 represents the rpm in x-axis and damped natural frequency in y axis. For different value of rpm, the corresponding natural frequencies are noted and the curve is obtained as shown above, the curve goes on increasing and it reaches a certain level above which the frequency becomes constant for further increase in RPM.

## COMPARISON WITH NATURAL FREQUENCY AND DAMPED NATURAL FREQUENCY

**Table 8.4: comparison table**

| Speed (RPM) | Natural frequency (Hz) | Damped natural frequency (Hz) |
|---|---|---|
| 1100 | 50.8 | 40.1 |
| 1250 | 104.6 | 94.8 |
| 1350 | 128.1 | 114.8 |
| 1450 | 129 | 117.8 |

International Journal of Applied Mathematics
Volume 38 No. 5s, 2025
ISSN: 1311-1728 (printed version); ISSN: 1314-8060 (on-line version)

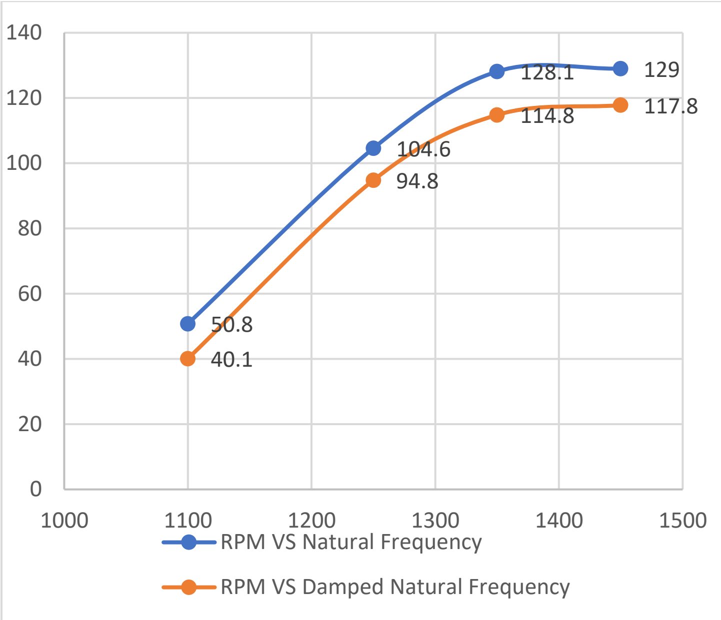


**Graph 8.7: Comparison between natural frequency and damped natural frequency**

**Damping ratio calculations:**

1.$F_d = f_n(1-\xi^2)^{0.5}$

a. $40.1=50.8(1-\xi^2)^{0.5}$

$\xi= 0.614$

b. $94.8=104.6(1-\xi^2)^{0.5}$

$\xi= 0.422$

c. $114.8=128.1(1-\xi^2)^{0.5}$

$\xi=0.443$

d. $117.8=129(1-\xi^2)^{0.5}$

$\xi=0.407$

## 7.Conclusion

The utilization of Fusion 360, a powerful computer-aided design (CAD) software, facilitated the fabrication process of the drone. With its comprehensive set of tools and features.

Furthermore, by incorporating an accelerometer into the vibration analysis, we were able to accurately measure and quantify the drone's vibration levels. This data allowed us to identify potential vibration-induced issues that could negatively impact the drone's performance or payload stability.

After implementing a damper, the natural frequency of the system has been reduced. In the graph, the reduction in natural frequency can be observed as a shift towards lower frequency values compared to the previous graph without the damper. This indicates that the damper effectively mitigates the system's vibrations and stabilizes its dynamic behavior. The reduction in natural frequency after using the damper suggests improved system stability and reduced susceptibility to resonance or unwanted vibrations. This outcome is desirable as it helps ensure the system operates within safe limits and minimizes the risk of structural damage or performance degradation.

## 8.Reference

[1] H. Xia, K. Yang, Y. Ma, Y. Wang, and Y. Liu, ''Noise reduction method 487 for acoustic sensor arrays in underwater noise,'' IEEE Sensors J., vol. 16, 488 no. 24, pp. 8972–8981, Dec.

**International Journal of Applied Mathematics**
**Volume 38 No. 5s, 2025**
ISSN: 1311-1728 (printed version); ISSN: 1314-8060 (on-line version)

2016, doi: 10.1109/JSEN.2016.2618770. 489

[2] H. Jingzhu, L. Dichen, L. Qingfen, Y. Yang, and L. Shanshan, ‘‘Electro- 490 magnetic vibration noise analysis of transformer windings and core,’’ IET 491 Electr. Power Appl., vol. 10, no. 4, pp. 251–257, Apr. 2016. 492

[3] T. Phway and A. J. Moses, ‘‘Magnetisation-induced mechanical resonan- 493 cein electrical steels,’’ J. Magn. Magn. Mater., vol. 316, no. 2, pp. 468–471, 494 2007. 495

[4] A. J. Moses, P. I. Anderson, and T. Phophongviwat, ‘‘Localized surface 496 vibration and acoustic noise emitted from laboratory-scale transformer 497 cores assembled from grain-oriented electrical steel,’’ IEEE Trans. Magn., 498 vol. 52, no. 10, pp. 1–15, Oct. 2016, doi: 10.1109/TMAG.2016.2584004. 499

[5] B. Zhang, N. Yan, J. Du, F. Han, and H. Wang, ‘‘A novel approach 500 to investigate the core vibration in power transformers,’’ IEEE Trans. 501 Magn., vol. 54, no. 11, pp. 1–4, Nov. 2018, doi: 10.1109/TMAG.2018. 5022839722. 503

[6] L. Min, S. Li, X. Zhang, F. Zhang, Z. Sun, M. Wang, Q. Zhao, Y. Yang, 504 and L. Ma, ‘‘The research of vibration monitoring system for trans- 505 former based on optical fiber sensing,’’ in Proc. IEEE 3rd Optoelectron. 506 Global Conf. (OGC), Sep. 2018, pp. 126–129, doi: 10.1109/OGC.2018. 5078529978. 508

[7] Y.-H. Chang, C.-H. Hsu, H.-L. Chu, and C.-P. Tseng, ‘‘Magnetomechanical 509 vibrations of three-phase three-leg transformer with different amorphous- 510 cored structures,’’ IEEE Trans. Magn., vol. 47, no. 10, pp. 2780–2783, 511 Oct. 2011, doi: 10.1109/TMAG.2011.2146242. 512

[8] M. Bagheri, A. Zollanvari, and S. Nezhivenko, ‘‘Transformer Fault 513 condition prognosis using vibration signals over cloud environment,’’ 514 IEEE Access, vol. 6, pp. 9862–9874, 2018, doi: 10.1109/ACCESS. 5152018.2809436. 516

[9] A. Secic, M. Krpan, and I. Kuzle, ‘‘Vibro-acoustic methods in the condition assessment of power transformers: A survey,’’ IEEE Access, vol. 7, 518 pp. 83915–83931, 2019, doi: 10.1109/ACCESS.2019.

Received: August 14, 2025 